Pressure effects on the resonant attenuation of soft porous beads-based materials for underwater acoustics

Thomas Lacour,[1] Romain Poupart,[2] Olivier Mondain-Monval,[2]
Christophe Aristégui,[1] Olivier Poncelet,[1] and Thomas Brunet[1, *]
[1] Univ. Bordeaux, CNRS, Bordeaux INP, I2M, UMR 5295, F-33400 Talence, France
[2] Univ. Bordeaux, CNRS, CRPP, UMR 5031, F-33600 Pessac, France

Dedicated coating materials for anechoism and furtivity in underwater acoustics must exhibit a strong reliability regarding their mechanical resistance to hydrostatic pressure. Soft porous materials, and especially, a distribution of soft porous beads within a polyurethane matrix have been previously proposed as an acoustic insulator device. The purpose of the present letter is to investigate the attenuation efficiency of soft porous silicone beads-based materials while being exposed to uniaxial loads mimicking hydrostatic pressures encountered in underwater acoustics. The acoustic performance of this locally resonant material is then compared to the classical coating technology using micro-balloons. The use of an adapted surfactant (a silicone alkyl polyether compound) in the fabrication process of the soft porous silicone-based beads, obtained through an emulsion templating process, leads to particles exhibiting an open porosity. The (resonant) attenuation of the soft porous beads-based material remains greater than the micro-balloons-based material until several bars. Above this critical resilience value, the mechanical stress irreversibly damages the soft porous beads.

I. INTRODUCTION

The design of innovative materials is of growing interest especially as a promising solution for underwater acoustic coatings [1, 2]. These thin materials are used in two situations: the first case deals with the stealth of submersible structures while the second case aims at anechoism [3]. To achieve both, the sound emitted (or reflected) by an immersed structure towards its environment has to be reduced significantly. For that purpose, the most common approach for underwater acoustic coatings is to fill a polyurethane (PU) matrix, that shows an ideal impedance matching with water, with micro-balloons that strongly enhance the scattering and the attenuation of the acoustic waves [4]. Those micro-balloons are micro-bubbles of gas with a typical size of about 40 µm encapsulated by polymeric shells. However, in the context of underwater acoustics, a serious concern is the collapse of these spherical inclusions and the buckling instability of their polymeric shells when the composite material is subjected to high hydrostatic pressures [5]. This buckling can affect seriously the acoustic properties of the coatings making them ineffective in terms of attenuation [6]. Other soft composite coatings involving simple air cavities have also shown a decrease in acoustic performances under hydrostatic pressures [7–9].

To circumvent this issue, an innovative solution is to cluster these air cavities within submillimetric solid beads made of soft porous silicone rubber with a very low speed of sound [10–12], as such composite materials exhibit a strong resonant attenuation. Those soft porous beads have a large number of applications [13] and can be produced using an emulsion templating approach [14]. In fact, it has been recently demonstrated that such emulsion-based materials could possess the ability to serve as acoustic insulators while dispersed in a PU matrix [15, 16]. Note that the porosity of these beads can be closed or open. As a matter of fact, the emulsion leading to the soft porous silicone rubber is composed of isolated droplets. During the drying step (i.e. the revelation of the porosity), the pores tend to collapse due to the drying pressure [17, 18]. Different ways have been proposed to circumvent that: either using supercritical carbon dioxide as a drying step [19], adding hydrogen peroxide in the emulsion formulation [19] or using another surfactant that leads to an open porosity [17]. Another benefit of soft porous beads is their ability to tune the frequency-dependent resonant attenuation since the increase in the size of the beads decreases the resonance frequency at which the attenuation reaches its maximum value [16]. Therefore, it is possible to lower the frequency at which the attenuation peak occurs down to the targeted frequency domain for underwater acoustics ($\sim$ kHz).

In this paper, we investigate the effect of hydrostatic pressure on the acoustic (resonant) attenuation of the two technologies: on the one hand, the micro-balloons commonly used in the naval industry and, on the other hand, our innovative soft porous beads. The pressure levels chosen, up to 10 and 20 bars, are aimed at mimicking an object diving to a depth of 100 and 200 meters.

II. ELABORATION OF THE COMPOSITE MATERIALS

A. Compounds

Silcolease UV Cata221, which is a 20 wt% alcoholic solution of (4-(1-methylethyl)phenyl)-(4-methylphenyl)iodonium

* thomas.brunet@u-bordeaux.fr

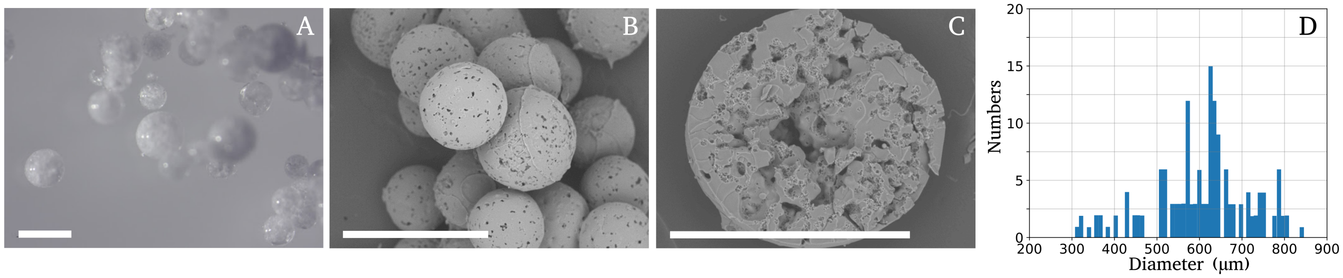

Figure 1. A. Optical microscopy of the soft porous beads. B. and C. SEM pictures of the soft porous beads showing their inner porosity (the white ruler correspond to 500 µm). D. Beads size distribution.

tetrakis(pentafluorophenyl)borate dissolved in propan-2-ol, and an epoxy-bearing PDMS rubber (Silcolease UV Poly200), has been kindly provided by Elkem Silicones. Isopropylthioxanthone (ITX, $\geq$99%) was supplied by Rahn. NaCl ($\geq$99%) has been purchased from Merck while ethanol (96%) is from Xilab. Silube J208-812 was kindly provided by Siltech Corporation. Glycerol (molecular biology) was ordered from Fisher Scientific. SikaBiresin® UR340 kit (isocyanate Part A and polyol Part B) from Sika was used to make the polyurethane matrix of the samples. Expancel 461 DET 40 d25 from Nouryon has been used as reference micro-balloons with a size of around 40 µm. 18.2 MΩ deionized water was filtered through a Milli-Q Plus purification pack.

B. Soft porous beads generation

Our samples are composite materials made of the same polyurethane matrix embedding inclusions, either soft porous beads or commercially available micro-balloons. The protocol to generate soft porous beads [17] has been described previously in the literature but here, slightly adapted. Briefly, a water-in-oil emulsion is obtained by the emulsification of 5.4 g of salted water (1.5 wt% of NaCl) as the dispersed phase in a continuous oil phase containing 12 g of Silcolease UV Poly200, 0.5 g of Silcolease UV Cata221, 10 mg of ITX and 50 mg of Silube J208-812. In this way, large double emulsion droplets are formed into a water phase. During their transit through a microfluidic device, the droplets of double emulsion are crosslinked via an UV lamp (Thorlabs) and then collected and washed with water and ethanol. They are then dried at 75 ^{o}C. The beads are characterized by scanning electron microscopy (SEM, Hitachi TM-1000) and optical microscopy (Nikon SMZ1270i) to extract the mean size through an optical analysis as shown in Fig. 1. The final porosity of the produced soft porous beads is about 30%.

The measured beads size distribution indicated a mean size of 598 $\pm$ 82 µm. The white color of the beads is due to the presence of pores at the micrometer scale thus scattering light. SEM pictures also evidence the interconnected porosity, as seen in Fig. 1-C.

C. Sample fabrication

Following the beads preparation, our two sets of composite samples are made using either the DET 40 micro-balloons or the soft porous beads by adding 2 and 6 vol%, respectively, of the inclusions in the polyurethane (SikaBiresin) to obtain the same final air quantity in the whole composite, and thus the same mass density for all the samples. The PU is a bi-component system composed of an isocyanate (part A) and a polyol (part B). Both parts are degassed during 30 min at 7 mbar prior to use. Inclusions are dispersed in 11 g of part B and this mixture is added into 22 g of part A. The resulting mixture is kept under stirring for 8 minutes prior to being poured in tailor-made PTFE molds with a diameter of 30 mm and a height of 4 and 6 millimeters. After being fully filled with the mixture and sealed, the molds are kept at 75 ^{o}C for 2 h. The top and the bottom of the mold are subsequently removed, leaving the sample inside the PTFE cylinder mold for acoustic analysis. Samples made of pure PU without any inclusions are also fabricated and will serve as reference materials.

III. ATTENUATION PERFORMANCE UNDER UNIAXIAL LOAD

Before mechanical tests, the intrinsic attenuation is measured for each unloaded sample as shown in Fig. 2. As previously reported [16], the attenuation of the pure PU matrix is very low at the ultrasonic frequency range considered here [0.1 - 1 MHz]. On the other hand, the acoustic attenuation is much higher in the sample containing soft porous beads compared to the one with micro-balloons, especially in a broad frequency range around 200 kHz for which the soft porous beads resonate [16]. As the micro-balloons-based material is the classical solution for underwater acoustics [20], the use of soft porous beads could be of crucial interest because of the large resonant attenuation they induce. In the following, acoustical tests are performed on all the samples to study the impact of an increasing static load on the acoustic attenuation of our materials at ultrasonic frequencies. Note that the (static) mechanical properties of these soft composite materials have already been exposed [21].

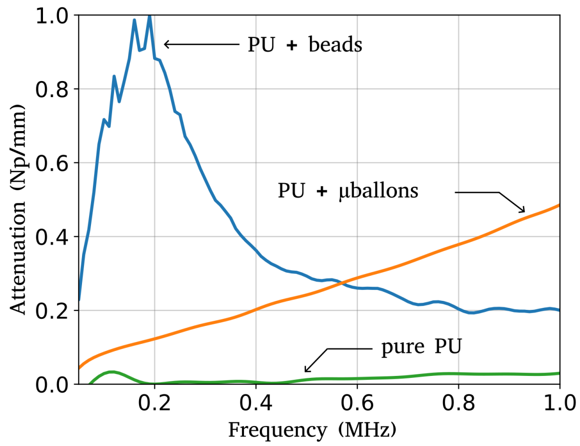

Figure 2. Compared evolutions of the (longitudinal-wave) attenuation as a function of frequency for the pure PU matrix (green), for sample containing micro-balloons (orange) and soft porous beads (blue).

A. High frequency measurements

First, acoustic measurements are reported at high ultrasonic frequencies. To perform the acoustic characterization under uniaxial compressional loads, cylindrical shaped samples were synthesized following the manufacturing process described in section II. The sample is confined within a hollow PTFE cylinder placed between two broadband ultrasonic transducers (emitter and receiver, Olympus V301) with a diameter of 30 mm and a central frequency of 500 kHz. This stacking was then placed into a traction/compression testing machine to ensure a purely uniaxial load. The mechanical compression is sustained thanks to a Zwick/Roell AllroundLine Z010 machine and its dedicated software TestExpert. During the mechanical tests, the samples may undergo several cycles of compression/relaxation, where the force applied on the samples was set up to 700 N corresponding to a static pressure of 10 bars. A nonzero initial force of few tens of newtons was first applied on the sample to ensure a reproducible contact area between each element of the stack over the different measurements done. For each applied force varying from 70 to 700 N, the transmitted acoustic signals were recorded with a constant step in force of 70 N (corresponding to an applied pressure step of 1 bar) for the non-absorbing pure PU sample and then for the material to be characterized (with micro-balloons or with soft porous beads). By comparing the transmitted spectra obtained for samples with and without particles, the (longitudinal-wave) attenuation can be easily retrieved for the composite materials, knowing the sample thicknesses, as shown in Fig. 3.

From these experimental results, one can draw meaningful conclusions. First, the attenuation of the sample containing the soft porous beads clearly decreases when the applied pressure increases as shown in Fig. 3-A. Moreover, the attenuation peak tends to shift slightly to higher frequencies. At around 8 bars, the attenuation is very low and almost no longer measurable as illustrated by the oscillations in the spectra that are due to multiple echoes reflecting on the two transducers, and thus interfering in the Fourier domain. This progressive decrease in the attenuation can be expected as the more compression goes, the higher it tends to close the porosity, thus leading to a dramatic reduction in the acoustic index contrast between beads and the surrounding matrix. The pressure release after this first ramp of applied loading on the sample does not allow the complete recovery of the initial attenuation level, as the attenuation is only about of 0.3 Np/mm at its maximum (Fig. 3-B) instead of the initial value of about 1 Np/mm. When the sample is submitted to additional pressure cycles, the attenuation continues to deteriorate because of the sample damage (Fig. 3-C) and cannot retrieve its initial level (before compression) even if the sample is left to rest for several days (Fig. 3-D).

It is worth noting that while the compressive strength of a polymeric foam decreased with increased interconnected pore ratio, the mechanical fatigue of the porosity is improved when opening the porosity [22]. It could be hypothesized that highly interconnected pores are equivalent to a unique large pore structure. The evidence of a critical pore size of porous PDMS below which the porosity tends to vanish has already been observed in the literature [18]. Indeed, optical microscopy observations performed before and after a cycle of compression/relaxation shows a disappearance of the whitish domains in the beads (see the insets of Fig. 3-A & B). Those domains are representative of the porosity, as the micrometer-sized pores promote the scattering of light at this scale. If the pores collapse, the beads lose their porosity and their sound speed is comparable to those in pure PDMS rubber ($\sim$1000 m/s instead of the 100 m/s for porous silicone rubber [10]). The sound speed (or acoustic index) contrast between the inclusions and the surrounding matrix becomes thus much lower since the sound speed in pure PU is about 1500 m/s. This diminution of the acoustic index leads to the vanishing of the resonant scattering attenuation of the material containing soft porous beads.

On the opposite, acoustic measurements performed on the sample containing micro-balloons show that this material seems to be more resistant to the applied force as shown in Fig 4-A & -B. In fact, the higher the pressure, the higher the acoustic attenuation. This behavior can be explained through the alteration of micro-balloon shells. Indeed, these objects are composed of a very thin polymeric shell that tends to buckle at high pressure making them ”softer”. If the micro-balloon shells become less rigid, the scattering strength of these air-filled particles

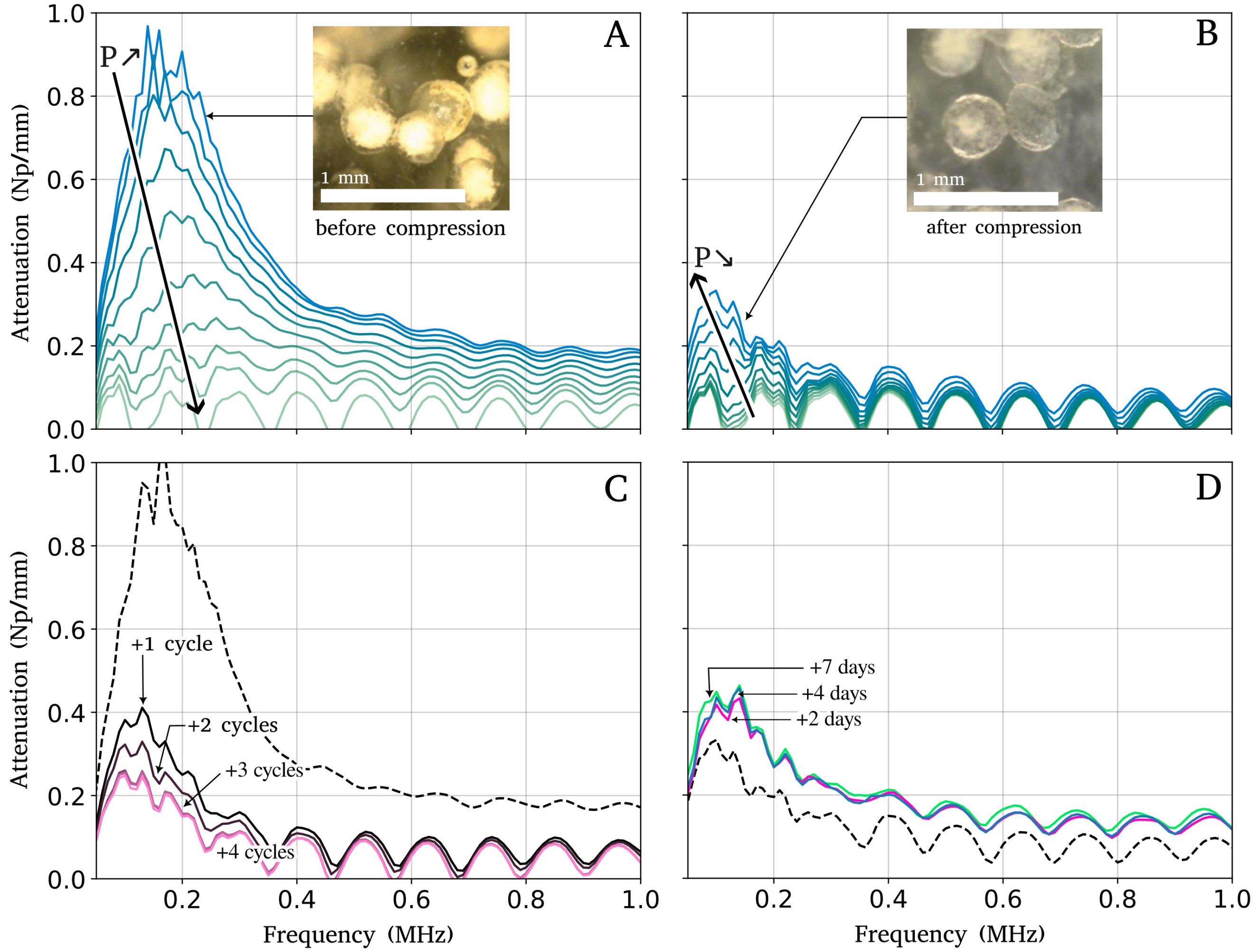

Figure 3. Evolution of the (longitudinal-wave) attenuation for the sample containing the soft porous beads, as a function of frequency for different static loads. The applied pressure increases from 1 to 10 bars by steps of 1 bar (A), and decreases down to 1 bar with the same steps (B). The sample is then subjected to several cycles of compression/relaxation (C) and is finally left to rest for several days (D).

increases leading to higher attenuation levels as previously discussed in similar materials. As predicted theoretically, the buckling of these shells may lead to a decrease of the effective elastic moduli of the composite [23]. The micro-balloons seem thus to be more appropriate to maintain a significant attenuation at high pressure but the material made of soft porous beads exhibit higher attenuation at low pressure that is due to particle resonances.

For naval underwater applications, working frequencies are about few tens of kHz and not hundreds of kHz as considered in the previous section. It is therefore worth considering whether the acoustic performance of the material made of soft porous beads also deteriorate under high applied pressures at lower frequencies.

B. Low frequency measurements

For these low-frequency measurements, other samples were elaborated with the same diameter but greater in height (30 mm and not few millimeters). The samples were confined in hollow PVC cylinders and placed within the Zwick/Roell machine between the two same broadband transducers used for the high-frequency measurements presented in the previous section. Here, the emitter was excited with a 5-cycle tone-burst centered at 50 kHz, which is the lowest frequency at which our ultrasonic transducers can generate and detect a measurable acoustic signal. A first series cycles of compression/relaxation, with a maximum applied pressure of 10 bars, was applied like in previous experiments.

In order to compare both technologies based on the soft porous beads and on the micro-balloons, the attenuation

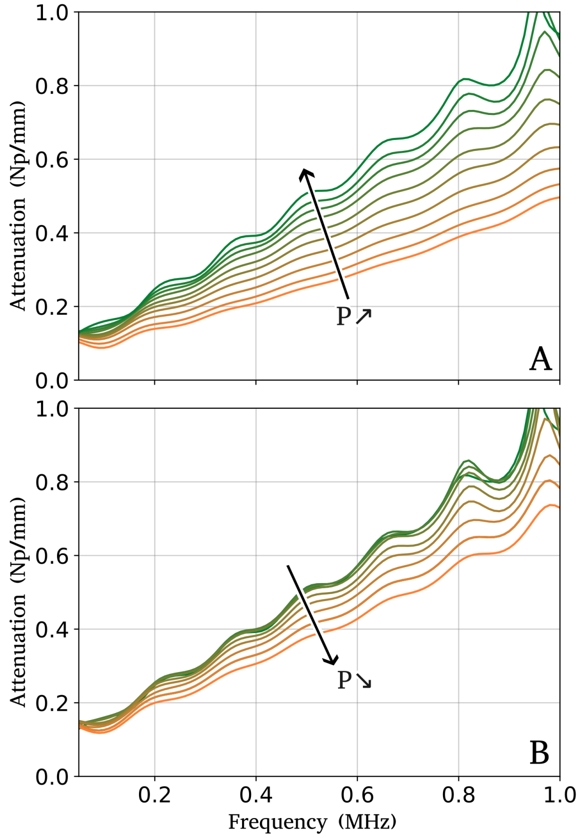

Figure 4. Evolution of the (longitudinal-wave) attenuation for the sample containing the micro-balloons, as a function of frequency for different static loads. The applied pressure increases from 1 to 10 bars by steps of 1 bar (A), and decreases down to 1 bar with the same steps (B).

difference

$$\Delta\alpha = \alpha_{\text{beads}} - \alpha_{\mu\text{-balloons}} \tag{1}$$

between the two materials is shown in Fig. 5-A for few successive cycles of compression/relaxation. Contrary to what has been shown for higher frequencies in the previous subsection, the sample containing the soft porous beads remains more absorbing at low frequency than the material made of micro-balloons, over the whole mechanical test since the attenuation difference $\Delta\alpha$ remains positive, even at 10 bars. Although the acoustic resonances tend to disappear under high applied pressures, some air cavities must remain in the soft porous beads (as seen in the inset of Fig. 3-B) maintaining a significant attenuation level.

Finally, a last series of cycles of compression/relaxation was conducted with higher pressure levels (Fig. 5-B). In this second series of ultrasonic experiments, the maximum force applied on the samples was 1400 N, corresponding to a hydrostatic pressure of 20 bars (and to an equivalent underwater depth of 200 m). Acoustic measurements shown in Fig. 5-B reveal that the soft porous

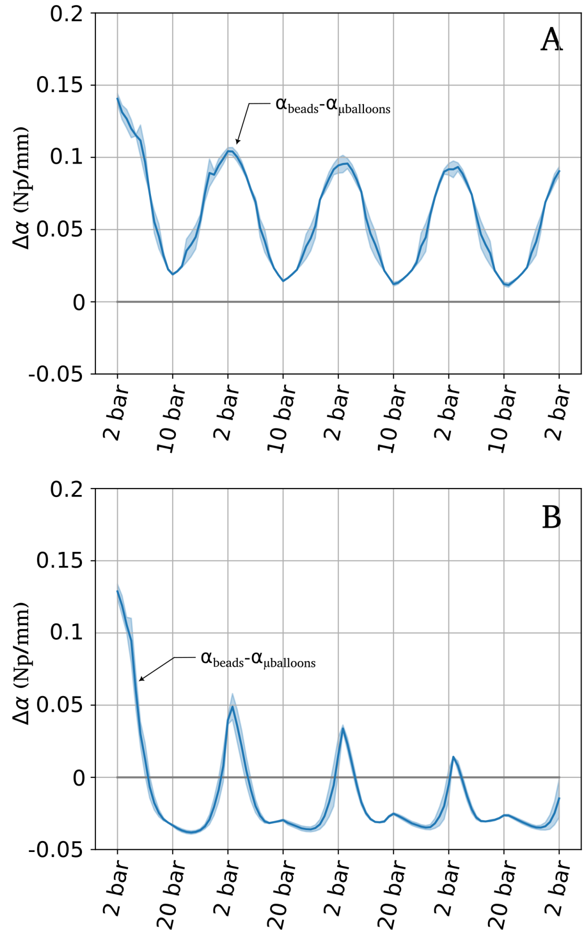

Figure 5. Evolution of the attenuation difference $\Delta\alpha = \alpha_{\text{beads}} - \alpha_{\mu-\text{balloons}}$ measured at 50 kHz over 4 cycles of compression/relaxation for applied pressure ranging from 2 bars up to 10 bars (A) or to 20 bars (B). The areas represent the repeatability of the experiments and the solid line corresponds to the mean value.

beads do not resist to these high pressures anymore since the attenuation difference becomes negative beyond 12 bars. Moreover, the damage inflicted to the material increases, leading to an irreversible fatigue as shown in the next cycles.

IV. CONCLUSIONS

To conclude, the composite materials made of soft porous beads randomly but uniformly dispersed in a polyurethane matrix exhibit interesting acoustic properties. At ambient pressure, its (resonant) attenuation is much higher than the one reached with the common technology used in naval industry based on micro-balloons. However, the resonance of soft porous beads is strongly impacted and lessened under static pressures because of the collapse of the beads porosity. Moreover, the initial resonant properties are not recovered after one or several cycles of compression/relaxation indicating that these mechanical tests irreversibly damage the structure of the soft porous beads. On the other hand, the composite materials made of micro-balloons demonstrate a much better pressure resistance that is probably due to the deformation of their shells. An alternative solution could be the reinforcement of the soft porous beads with a shell, mimicking the micro-balloons technology while keeping the advantages of the air-cavities clusterization in resonant particles. The mechanical reinforcement of the (soft) matrix could be also an efficient way to limit the collapse of such porous and compressible material.

ACKNOWLEDGMENTS

TL, RP and all the coworkers are indebted to the ANR and DGA for granting them a postdoctoral position through the PANAMA Project (ANR-17-ASTR-0002). Fruitful conversations with J. Leng, from LOF; F. Le Lay, P. Rublon, J. Delcroix and Y. Renou from Naval Group are gratefully acknowledged. The authors thank Siltech Company for providing them with the Silube surfactant and also F. Marchal and T. Ireland from Elkem Silicones for providing them with silicone rubber and cationic initiator. They also thank J. Guitard for his assistance with the Zwick/Roell machine, A. Turani-i-Belloto for providing the MATLAB program used for the size distribution and V. Mouille & J.-E. Maigne for some additional acoustical experiments.

DATA AVAILABILITY

The data that support the findings of this study are available from the corresponding author upon reasonable request.

[1] W. Sun, X. Yan, and X. Zhu, Journal of Applied Polymer Science **122**, 2359 (2011).
[2] Y. Fu, I. I. Kabir, G. H. Yeoh, and Z. Peng, Polymer Testing **96**, 107115 (2021).
[3] P. Méresse, C. Audoly, C. Croënne, and A.-C. Hladky-Hennion, Comptes Rendus Mécanique **343**, 645 (2015).
[4] B. R. Matis, S. W. Liskey, N. T. Gangemi, Z. J. Waters, A. D. Edmunds, W. B. Wilson, D. M. Photiadis, B. H. Houston, and J. W. Baldwin, Langmuir **36**, 5787 (2020).
[5] G. Gaunaurd, E. Callen, and J. Barlow, The Journal of the Acoustical Society of America **76**, 173 (1984).
[6] S. Beretti, in *10ème Congrès Français d'Acoustique* (2010).
[7] M. Thieury, A. Tourin, J. Dassé, and V. Leroy, in *13th International Congress on Artificial Materials for Novel Wave Phenomena* (2019).
[8] M. Thieury, V. Leroy, J. Dassé, and A. Tourin, Journal of Applied Physics **128**, 135106 (2020).
[9] H. Yang, H. Zhao, and J. Wen, Journal of Sound and Vibrations **533**, 116985 (2022).
[10] K. Zimny, A. Merlin, A. Ba, C. Aristégui, T. Brunet, and O. Mondain-Monval, Langmuir **31**, 3215 (2015).
[11] T. Brunet, A. Merlin, B. Mascaro, K. Zimny, J. Leng, O. Poncelet, C. Aristégui, and O. Mondain-Monval, Nature materials **14**, 384 (2015).
[12] A. Ba, A. Kovalenko, C. Aristégui, O. Mondain-Monval, and T. Brunet, Scientific Reports **7**, 1 (2017).
[13] M. T. Gokmen and F. E. Du Prez, Progress in polymer science **37**, 365 (2012).
[14] M. S. Silverstein, Progress in Polymer Science **39**, 199 (2014).
[15] H. Zhou, B. Li, and G. Huang, Journal of Applied Polymer Science **101**, 2675 (2006).
[16] R. Poupart, T. Lacour, P. Darnige, O. Poncelet, C. Aristégui, T. Voisin, S. Marre, T. Brunet, and O. Mondain-Monval, RSC advances **10**, 41946 (2020).
[17] A. Kovalenko, K. Zimny, B. Mascaro, T. Brunet, and O. Mondain-Monval, Soft matter **12**, 5154 (2016).
[18] P. T. A. Nguyen, M. Vandamme, and A. Kovalenko, Soft Matter **16**, 9693 (2020).
[19] R. Kumar, Y. Jin, S. Marre, O. Poncelet, T. Brunet, J. Leng, and O. Mondain-Monval, Journal of Porous Materials **28**, 249 (2021).
[20] C. Audoly, in *Journal of Physics: Conference Series*, Vol. 353 (IOP Publishing, 2012) p. 012004.
[21] D. Zeka, A. Catapano, P. Mariano, M. Montemurro, R. Poupart, J. Mondain-Monval, O.and Delcroix, and R. P., Materials & Design **168**, 104276 (2022).
[22] C. Zhang, J. Li, Z. Hu, F. Zhu, and Y. Huang, Materials & Design **41**, 319 (2012).
[23] R. De Pascalis, I. D. Abrahams, and W. J. Parnell, Journal of the Mechanics and Physics of Solids **61**, 1106 (2013).